Vacuum 203 (2022) 111302

Contents lists available at ScienceDirect

Vacuum

journal homepage: www.elsevier.com/locate/vacuum

# Photoconductivity study of $Ca_2Si$ epitaxial film on Si(111) substrate

Nikita Siminel [a,*], Konstantin N. Galkin [b], Ernest Arushanov [a], Nikolay G. Galkin [b]

[a] Institute of Applied Physics, Ministry of Education and Research of the Republic of Moldova, Chisinau, MD, 2028, Republic of Moldova
[b] Institute of Automation and Control Processes FEB RAS, 5 Radio St, 690041, Vladivostok, Russia

ARTICLE INFO

*Keywords:*
$Ca_2Si$ film
Si(111) substrate
Epitaxy
Photoconductivity
Band gap nature
Temperature dependence
Electron-phonon interactions
Modelling

ABSTRACT

Semiconductor calcium semi-silicide ($Ca_2Si$) with a complex crystal and energy band structure is theoretically characterized by a direct fundamental transition, which is difficult to identify experimentally in $Ca_2Si$ films due to high absorption at defect levels. The study of the temperature dependences of photoconductivity in $Ca_2Si$ epitaxial films is one of the methods for assessing both the nature of the fundamental transition and a number of thermodynamic parameters. In this work, photoconductivity was firstly observed in an epitaxial $Ca_2Si$ film grown on a Si(111) substrate in the temperature range from 10 K to 300 K. Based on an analysis of the parameters of three thermodynamic models, the existence of a direct fundamental transition $E_g = 1.195$ eV at 0 K was proved, and the effective phonon energy ($<E_{ph}>$), the Einstein ($\Xi$) and Debye ($\Theta_D$) temperatures, as well as the electron-phonon coupling constant, and the hole mobility were determined.

## 1. Introduction

Semiconductor silicides of alkaline earth metals (Ca, Mg, Ba) attract considerable attention as promising materials for thermoelectric converters [1]. Among these elements, calcium (Ca) is one of the most common elements on Earth and occupies 5th place in their total distribution [2]. Calcium silicides form six compounds with different crystal structures and compositions [3] and have a wide range of properties from semiconductor [4,5] to semimetallic from theoretical [6] and experimental points of view [7–11]. Interest in $CaSi_2$ with a direct gap ranging, according to *ab-initio* theoretical calculations, from 0.30 to 0.36 eV [12–14] to 1.02 eV [4] is connected mainly to its possible incorporation into existing silicon technologies and utilization in microelectronic devices [15].

Transport properties of $Ca_2Si$ thin films, including the resistivity $\rho(T)$ and the Hall coefficient $R(T)$, were studied, and an effective mobility of about 300 $cm^2/Vs$ was estimated [15–17]. The band gap determined from the data of the *in situ* Hall temperature measurements of two-dimensional $Ca_2Si$ layer grown on Si(111) substrate [17] was found to be equal to 1.02 eV, which is consistent with *ab-initio* calculations in the quasiparticle approach within the framework of the GW approximation [4].

From the transmission and reflection spectra of the grown samples, it was found that $Ca_2Si$ film has a first direct interband transition at $E_{1d} = 1.095 \pm 0.15$ eV [18], strong defect adsorption lower 1.0 eV and dispersionless refractive index $n_o \leq 3.8$. Eight Raman peaks and 6 FIR peaks were first registered and identified, which are in good agreement with the experimental study [18] and theoretical calculations [19]. Although $Ca_2Si$ is a semiconductor compound according to first-principle theoretical calculations [4,7–9] and experimental data [18,19], carrier photogeneration in it has not been previously studied.

In this study, we report on band gap energy and temperature-dependent photoconductivity (PC) measurements of $Ca_2Si$ epitaxial film grown on $Mg_2Si$/Si(111) system. The value of the band gap is determined from PC measurements and the temperature dependence of the direct gap was studied using three different models, namely the three-parameter thermodynamic model of O'Donnell and Chen [20], the Einstein model [21] and the Pässler model [22].

## 2. Experimental procedure

### 2.1. Thin film and device structure preparation

Experiments on the growth of $Ca_2Si$ films on a substrate with (111) orientation were carried out in the ultrahigh-vacuum (UHV) chamber of the OMICRON Compact setup, the analytical and technical equipment of which was described in previous work [18]. The growth of the $Ca_2Si$ films consisted of three stages [18]: (1) formation of a sacrificial $Mg_2Si$ layer by reactive deposition epitaxy (RDE) at 150 °C; (2) formation of a $Ca_2Si$ seed layer by RDE at 250 °C and (3) growth of a thick $Ca_2Si$ film

* Corresponding author.
*E-mail addresses:* nikita.siminel@ifa.md, siminel.n@gmail.com (N. Siminel).

https://doi.org/10.1016/j.vacuum.2022.111302
Received 12 April 2022; Received in revised form 2 June 2022; Accepted 28 June 2022
Available online 1 July 2022

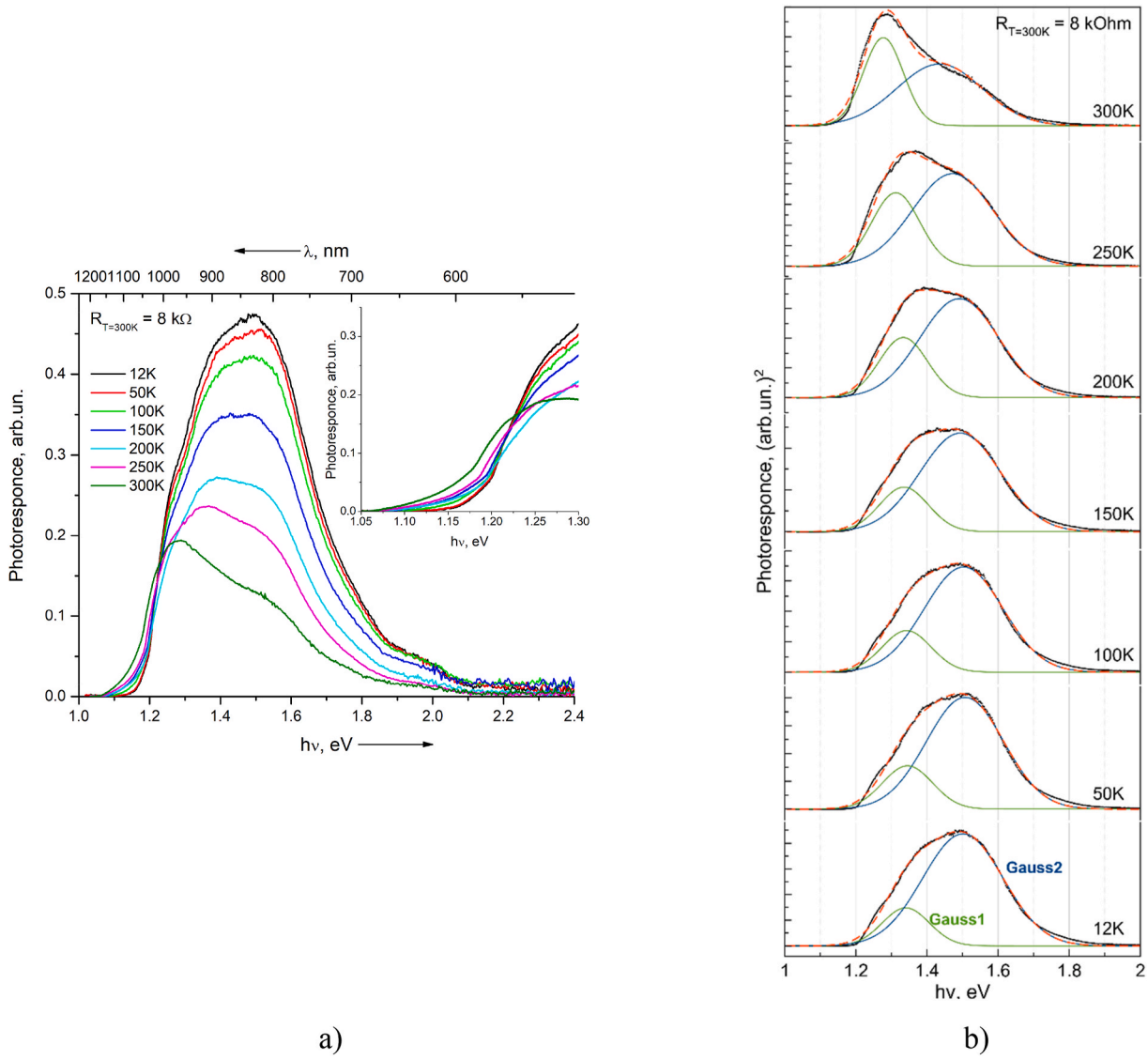


**Fig. 1.** a) Temperature dependence of the near-band-edge PC spectra for $Ca_2Si$/Si system; b) Deconvolution of quadratic relation of PC for $Ca_2Si$/Si system.

(100 nm) by molecular beam epitaxy (MBE) at 250 °C. The morphology and structure of the grown $Ca_2Si$ films on Si(111) substrate were studied for samples ***A***, ***B*** and ***C*** by AFM and XRD methods in detail in Ref. [18]. After the samples were unloaded from the UHV chamber, aluminum (Al) pads were applied to them through a contact mask and annealed in a special vacuum chamber, then the Hall cross structure was etched, and Al wires (20 μm thick) were subjected to ultrasonic welding to the contact pads in an unclosed microcircuit package. The resulting device structures were used for low-temperature measurements of the conductivity and photoconductivity of the grown films.

### 2.2. Photoconductivity measurements

The PC of the studied compound was measured using a custom setup consisting of a monochromator, close-circuit helium cryostat and lock-in amplifier. A halogen light source with a Tungsten filament connected to a monochromator provided discrete wavelengths in the range of 500–1200 nm (1.03–2.48 eV). Monochromatic light rays were modulated with a mechanical chopper at 12 Hz and were focused on the surface of the sample. The output photocurrent signal was collected as the voltage drop on a load resistance *R* which was equal to the resistance of the sample at room temperature. In the case of $Ca_2Si$, the load resistance was 8 kΩ. The signal was collected and analysed by the lock-in amplifier. Temperature evolution of the PC was measured in the temperature range of 12 K–300 K. The PC spectra are calibrated by the spectral constant of the setup, which accounts for characteristic spectra of the monochromator, tungsten lamp, and slit width.

## 3. Results and discussion

In Fig. 1(a) temperature dependence of PC spectra is shown for $Ca_2Si$/Si system in sample ***A*** grown in Ref. [18]. At every temperature, the PC spectrum is composed of two peaks, which becomes evident after deconvolution with Gauss curves (Fig. 1 b). Positions of these peaks at 12 K are 1.34 eV and 1.50 eV, however, at 300 K, both peaks shift toward lower energy positioning at 1.28 eV and 1.43 eV respectively. It is also worth noting that temperature change causes energy transfer between these two states. The intensity of respective peaks changes alternately at low and high temperatures. A comparison of the PC spectra of the $Ca_2Si$/Si system and a pure Si substrate (not shown) over the entire temperature range, showed that the PC signal of the Si substrate is approximately one order of magnitude weaker than that of $Ca_2Si$/Si system in the energy range of 1.2–1.8 eV. Change in the spectral composition at 1.2–1.4 eV suggests that predominant contribution to the

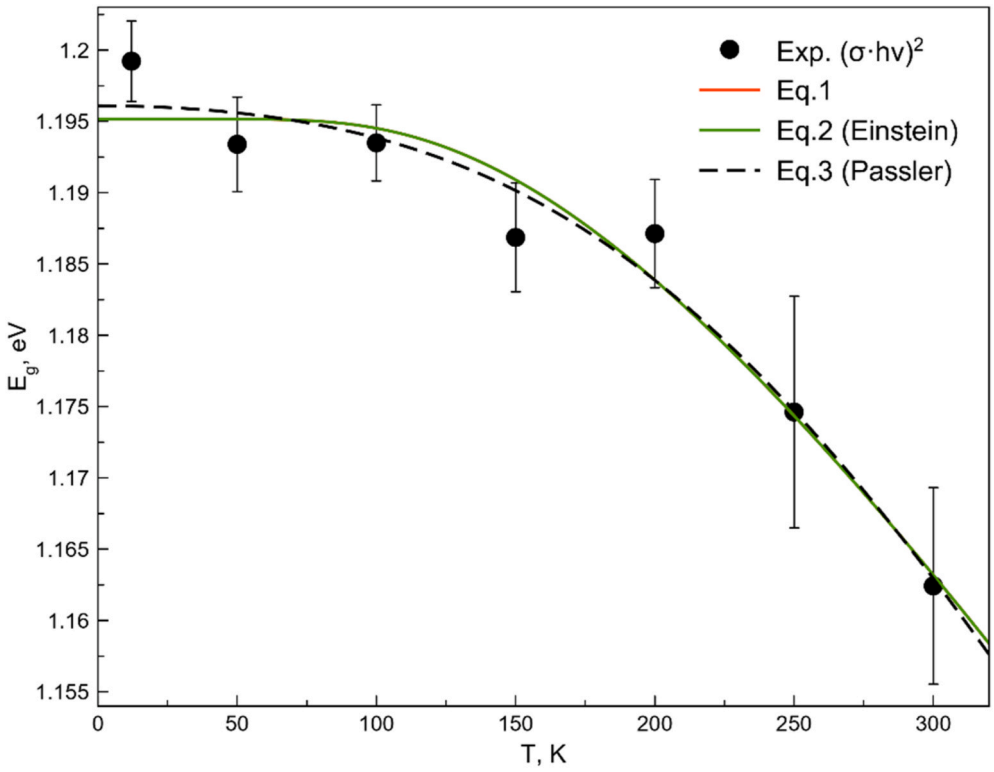


**Fig. 2.** Experimental band gap energy vs. temperature for $Ca_2Si$. Black dots – experimental data $(\sigma h\nu)^2$; lines – fitting based on models (1), (2) and (3).

PC signal of the $Ca_2Si$/Si system is provided by $Ca_2Si$ film.

The obscure point of the studied compound is whether it is possible to consider epitaxial films of $Ca_2Si$ as direct or indirect gap semiconductor with a band gap of about 1.0 eV according to *ab-initio* quasiparticle calculations [4] and experimental study [17].

The fundamental absorption edge in a semiconductor is proportional to the absorption coefficient [23], and the type of fundamental transition determines the dependence of the absorption coefficient on the photon energy ($h\nu$), which specifies band gap type - direct or indirect. It is then possible to determine the band gap [24] and its temperature dependence from the PC spectrum measured in a wide temperature range. Assuming a direct band gap the band gap energies of the $Ca_2Si$ semiconductor were estimated by extrapolating the linear portion of PC graphs of $(\sigma h\nu)^2$ versus $h\nu$ to zero [24] (Fig. 2 – black dots). Following Ref. [25] the temperature dependence of the direct gap was studied using three different models, the three-parameter thermodynamic model of O'Donnell and Chen [20], the Einstein model [21] and the Pässler model [22].

Firstly, O'Donnell and Chen stated that the temperature-dependent electron-phonon interactions effectively determine semiconductor bandgaps. The band gap reflects the bond energy. An increase in temperature changes the chemical bonding as electrons are promoted from the valence band to the conduction band [20]. The electron-phonon interaction, in this case, is dominant and can be described by a three-parameter thermodynamic model:

$$E_g(T) = E_g(0) - S \cdot E_{ph}\left[coth\left(\frac{E_{ph}}{2kT}\right) - 1\right], \quad (1)$$

where $E_g(0)$ is the bandgap at $T = 0$ *K*, $E_{ph}$ is effective phonon energy, and $S$ is a dimensionless constant related to the electron-phonon coupling. This thermodynamic model provides a good description of $E_g(T)$ for various semiconducting materials [25].

Second, in the Einstein model, the $E_g(T)$ dependence can be expressed by the following equation [21]:

**Table 1**
Parameters calculated using models (1), (2), and (3) that approximate band gap temperature relation from PC of $Ca_2Si$.

| | Parameters | |
|---|---|---|
| Eq. (1) | $E_g(0)$, *eV* | 1.195 ± 0.002 |
| | $<E_{ph}>$, *meV* | 48.3 ± 1.8 |
| | $S$ | 1.819 ± 0.17 |
| Eq. (2) (Einstein model) | $E_g(0)$, *eV* | 1.195 ± 0.002 |
| | $K$, *eV* | 0.175 ± 0.14 |
| | $\Xi$, *K* | 561 ± 212 |
| Eq. (3) (Pässler model) | $E_g(0)$, *eV* | 1.196 ± 0.002 |
| | $\alpha$, *meV K*$^{-1}$ | 14.21 ± 5.87 |
| | $\Theta$, *K* | 2734 ± 854 |
| | $r$ | 0.048 ± 0.022 |

$$E_g(T) = E_g(0) - K(e^{\frac{\Xi}{T}} - 1)^{-1}, \quad (2)$$

where $K$ is a temperature-independent constant and $\Xi$ is the Einstein temperature.

Thirdly, eq. (3) provides a good approximation of the analytical description of $E_g(T)$ proposed by Pässler [22], in the case when electron-phonon interaction is dominant. It is worth mentioning that this form of the Pässler equation represents a reasonable approximation for $r > 0.15$.

$$E_g(T) = E_g(0) - \alpha\left(\frac{\Theta}{2}\right)\left[\left(1 + 2r\left(\frac{2T}{\Theta}\right)^2 + \left(\frac{2T}{\Theta}\right)^4\right)^{\frac{1}{4}} - 1\right] \quad (3)$$

The temperature relation of experimental $E_g$, calculated from extrapolation of PC curves, and the fitting plots of the three-parameter thermodynamic model, the Einstein model and the Pässler model are given in Fig. 2. The fitting plots of all models predict experimental results reasonably well. For all models, the coefficient of determination,

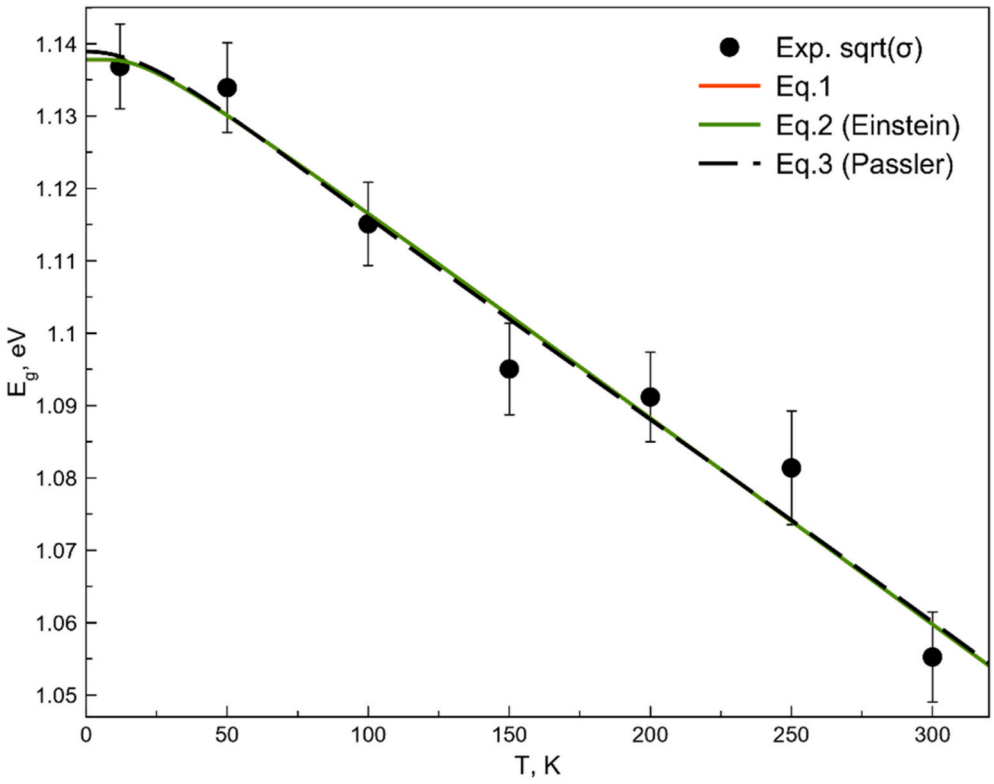


**Fig. 3.** Experimental band gap energy vs. temperature for $Ca_2Si$ calculated in $\sqrt{\sigma}$ coordinates. Black dots — experimental data, solid lines — fitting based on models (1), (2), and (3).

which ascertains the fitting accuracy, is greater than 0.9750. The obtained fitting parameters are summarised in Table I.

By fitting experimental data to eq. (1) and eq. (2) the following set of parameters were obtained: $E_g(0) = 1.195$ eV, $<E_{ph}> = 48.3 \pm 1.8$ meV, $S = 1.819 \pm 0.17$, $K = 0.175$ and Einstein temperature 561 K. The latter are close to the Debye temperature reported for Si (600 K) [27] and silicides $Mg_2Si$ (432 K) [28], $CrSi_2$ (793 K) [29] and $FeSi_2$ (640 K) [30]. The determined width of the direct band gap at room temperature (1.195 eV) agrees well with the of optical spectroscopy band gap data (1.095 eV) for $Ca_2Si$ films grown by this technology [18].

Our value of the electron-phonon coupling parameter $S$ is higher than the reported value for Si (1.49) [20,26] and lower than that for III–V compounds like InP (1.94) [21,31], GaAs (3.0) and GaP (3.35) [20, 26]. It can be concluded that the interaction between band-edge states and the phonon system in $Ca_2Si$ is stronger than in silicon and not so strong as in indium or gallium phosphides and arsenides [25].

Pässler's model is not valid in our case. The value of $r$ is much smaller than 0.15. From Eq. (1) or Eq. (2) we can write [26]:

$$\frac{dE_g}{dT} = -\frac{SE_{ph}^2}{2kT^2 \sinh^2\left(E_{ph}/2kT\right)} \tag{4}$$

At high temperatures, $k_BT \gg E_{ph}$ and the slope of the $E_g$ vs $T$ curve approaches its limiting value [26]:

$$-\left[\frac{dE_g}{dT}\right]_{max} = 2Sk_B \tag{5}$$

Comparing the above given $T \to \infty$ asymptote of Eq. (1) or Eq. (2) with its counterpart due to equation (2), the following correlations between the different model parameters are found:

$2Sk_B = K/\Xi = \delta$ for the magnitude of the limiting slope and $E_{ph}/k_B = \Xi = \Theta_D$ for the effective phonon temperature [25]. Comparing the parameter values listed in Table I, we conclude that, within deviations of less than 5%, these theoretical relations are fulfilled for the three-parameter thermodynamic model and the Einstein model, and not for the Pässler model.

**Table 2**
Parameters calculated using models (1), (2), and (3) that approximate band gap temperature relation from PC of $Ca_2Si$.

| | Parameters | |
|---|---|---|
| Eq. (1) | $E_g(0)$, eV | 1.137 ± 0.007 |
| | $<E_{ph}>$, meV | 4.8 ± 7.6 |
| | $S$ | 1.66 ± 0.23 |
| Eq. (2) (Einstein model) | $E_g(0)$, eV | 1.137 ± 0.007 |
| | $K$, eV | 0.016 ± 0.027 |
| | $\Xi$, K | 56 ± 88 |
| Eq. (3) (Pässler model) | $E_g(0)$, eV | 1.139 ± 0.008 |
| | $\alpha$, meV $K^{-1}$ | 0.323 ± 0.067 |
| | $\Theta$, K | 247 ± 668 |
| | $r$ | 3.58 ± 4.56 |

Assuming that mobility $\mu$ is determined by lattice scattering, its value can be expressed by [25,32].

$$\mu = \frac{48}{9\pi}\left[\frac{3}{4\pi}\right]^{1/3}\left[\frac{\pi}{2}\right]^{1/2}\frac{e\hbar^2 k}{(\Omega)^{1/3} m^{*3/2}(kT)^{3/2}\partial E_g/\partial T}, \tag{6}$$

where $\Omega$ is the volume of the unit cell and $m^*$ is the effective mass. The hole mobility was calculated by assuming that the hole effective mass $m_h/m_0 = 1.0$. At room temperature, we estimate hole mobility of $\mu = 98$ $cm^2/Vs$ (by applying the thermodynamic model and the Einstein model). The value is lower than that reported for the room temperature effective Hall mobility value [17].

The band gap energies of $Ca_2Si$ were also estimated by extrapolating the linear portion of PC graphs of $\sqrt{\sigma}$ versus $h\nu$ to zero [24] assuming that $Ca_2Si$ could be possible indirect gap material. Fig. 3 shows such a

relation of $E_g$ with temperature. Similar to the previous case, three different models were used to approximate the temperature relation of the band gap. The obtained fitting parameters are given in Table II.

Both, the thermodynamic and the Einstein model very underestimate the effective phonon energy and Einstein temperature. As far as Pässler model is concerned by fitting equation (3) to our data of $E_g(T)$, the following set of parameters is obtained: $E_g(0) = 1.139$ eV, $\Theta = 247$ K, $r = 3.58$, and $\alpha = 0.323$ meV K$^{-1}$ (Table II). However, the Pässler model restrictive requirement namely $r$ lower than $\pi^2/12$ is not valid for the case of our $Ca_2Si$ data. It means that the model could not be applied to $Ca_2Si$ $E_g(T)$ data.

We can conclude that both the three-parameter models are good enough to fit the experimental $E_g(T)$ data within the accuracy of the measurement assuming that $Ca_2Si$ is direct gap material. The four-parameter Pässler model is not valid in our case. Analysis of $E_g(T)$ was done in assuming that $Ca_2Si$ is an indirect or direct gap compound. The latter shows reasonable results in contrast to that of the former one. It can be considered as ancillary confirmation of the direct gap nature of $Ca_2Si$.

## 4. Conclusions

The photoconductive measurements of $Ca_2Si$/Si system have been carried out. The temperature dependence of the direct band gap in $Ca_2Si$ film in the temperature range of 12–300 K, was studied by using a three-parameter thermodynamic model, the Einstein model and the Pässler model. The first two models showed reasonably good fits to experimental data on temperature variation of the band gap in the case of the $Ca_2Si$ direct gap approach. The values of the band gap at $T = 0$ K, a dimensionless constant related to the electron-phonon coupling and an estimation for the room-temperature hole mobility of $Ca_2Si$, have been derived from the applied models. The latter are within the experimental accuracy of the data, and show a good overlap between estimated data from the fitting parameters and experimental data and data in the literature.

## CRediT authorship contribution statement

**Nikita Siminel:** Writing – original draft, Software, Investigation, Formal analysis. **Konstantin N. Galkin:** Writing – review & editing, Formal analysis, Conceptualization. **Ernest Arushanov:** Writing – review & editing, Supervision, Project administration, Methodology, Data curation, Conceptualization. **Nikolay G. Galkin:** Writing – review & editing, Methodology, Investigation, Funding acquisition, Data curation, Conceptualization.

## Declaration of competing interest

The authors declare that they have no known competing financial interests or personal relationships that could have appeared to influence the work reported in this paper.

## Data availability

Data will be made available on request.

## Acknowledgments

This work was carried out with financial support from the Russian Foundation for Basic Research grant (No. 20-52-00001-Bel_a). The authors thank PhD E.A. Chusovitin and young researcher E. Yu. Subbotin for preparing the test integrated structure and ultrasonic compression of Al contacts to the $Ca_2Si$ film for low-temperature measurements of conductivity and photoconductivity and Dr. Sci. D.L. Goroshko - for fruitful discussions.

## References

[1] V.K. Zaitsev, M.I. Fedorov, I.S. Eremin, E.A. Gurieva, in: D.M. Rowe (Ed.), Thermoelectrics Handbook Macro to Nano, 2006.
[2] F.W. Clarke, The relative abundance of the chemical elements, Phil. Soc. Washington Bull. 11 (1889) 135–141.
[3] P. Manfrietti, M.L. Fornasini, A. Palenzona, The phase diagram of the Ca-Si system, Intermetallics 8 (2000) 223–228, https://doi.org/10.1016/S0966-9795(99)00112-0.
[4] S. Lebegue, B. Arnaud, M. Alouani, Calculated quasiparticle and optical properties of orthorhombic and cubic $Ca_2Si$, Phys. Rev. B 72 (2005), 085103, https://doi.org/10.1103/PhysRevB.72.085103.
[5] A. Moll, R. Viennois, P. Hermet, A. Haidoux, J.-L. Bantignies, M. Beaudhuin, Stability and properties of the friendly environmental Zintl phases: $Ca_3Si_4$ and $Ca_{14}Si_{19}$, Acta Mater. 125 (2017) 490–497, https://doi.org/10.1016/j.actamat.2016.12.023.
[6] O. Bisi, L. Braikovich, C. Carbone, I. Lindau, A. Iandelli, G.L. Olcese, A. Palenzona, Chemical bond and electronic states in calcium silicides: theory and comparison with synchrotron-radiation photoemission, Phys. Rev. B 40 (1989) 10194–10202, https://doi.org/10.1103/PhysRevB.40.10194.
[7] M. Aoki, N. Ohba, T. Noritake, S. Towata, Reversible hydriding and dehydriding properties of CaSi: potential of metal silicides for hydrogen storage, Appl. Phys. Lett. 85 (2004) 387, https://doi.org/10.1063/1.1773930.
[8] M. Affronte, O. Laborde, G.L. Olcese, A. Palenzona, Low temperature properties of calcium mono- and disilicides, J. Alloys Compd. 274 (1–2) (1998) 68–73, https://doi.org/10.1016/S0925-8388(98)00570-2.
[9] N.G. Galkin, K.N. Galkin, A.V. Tupkalo, Z. Fogarassy, B. Pécz, A low temperature growth of Ca silicides on Si(100) and Si(111) substrates: formation, structure, optical properties and energy band structure parameters, J. Alloys Compd. 813 (15) (2020), 152101, https://doi.org/10.1016/j.jallcom.2019.152101.
[10] T. Terada, T. Ishibe, T. Katayama, K. Sato, T.Q. Nguyen, H. Nakano, Y. Nakamura, Thermoelectric power factor enhancement of calcium-intercalated layered silicene by introducing metastable phase, APEX 14 (2021) 11, https://doi.org/10.35848/1882-0786/ac2a57.
[11] T. Terada, Y. Uematsu, T. Ishibe, N. Naruse, K. Sato, T. Nguyen, E. Kobayashi, H. Nakano, Y. Nakamura, Giant enhancement of seebeck coefficient by deformation of silicene buckled structure in calcium-intercalated layered silicene film, Advances Materials Interfaces 9 (1) (2022), 2201752, https://doi.org/10.1002/admi.202101752.
[12] D.B. Migas, L. Miglio, V.L. Shaposhnikov, V.E. Borisenko, Comparative study of structural, electronic and optical properties of $Ca_2Si$, $Ca_2Ge$, $Ca_2Sn$ and $Ca_2Pb$, Phys. Rev. B 67 (2003), 205203, https://doi.org/10.1103/PhysRevB.67.205203.
[13] J. Hu, A. Kato, T. Sadoh, Y. Maeda, K.N. Galkin, T.V. Turchin, N.G. Galkin, H. Tatsuoka, Optical and electronic properties of $M_2Si$ (M = Mg, Ca and Sr) grown by reactive deposition technique, Int. J. Mod. Phys. B 24 (2010) 4639, https://doi.org/10.1142/S0217979210056657. Corrigendum of International Journal of Modern Physics B 24 (2010) 3693–3699.
[14] D.B. Migas, V.O. Bogorodz, A.B. Filonov, V.L. Shaposhnikov, V.E. Borisenko, N. G. Galkin, Electronic properties of semiconducting $Ca_2Si$ silicide: from bulk to nanostructures by means of first principles calculations, Jpn. J. Appl. Phys. 54 (2015), 07JA03, https://doi.org/10.7567/JJAP.54.07.JA03.
[15] N.G. Galkin, K.N. Galkin, I.M. Chernev, D.L. Goroshko, E.A. Chusovitin, A. V. Shevlyagin, A.A. Usenko, V.V. Khovailo, Comparison of the structural, optical and thermoelectrical properties of Ca silicide films with variable composition on Si substrates, Defect Diffusion Forum 386 (2018) 3–8. https://doi.org/10.4028/www.scientific.net/DDF.386.310/4028/www.scientific.net/DDF.363.3.
[16] L. Dermenji, K.G. Lisunov, K.N. Galkin, D.L. Goroshko, E.A. Chusovitin, N. G. Galkin, E. Arushanov, Transport properties of $CaSi_2$ and $Ca_2Si$ thin films, Solid State Phenom. 312 (2020) 3–8. https://doi.org/10.4028/www.scientific.net/SSP.312.3.
[17] S.A. Dotsenko, D.V. Fomin, K.N. Galkin, D.L. Goroshko, N.G. Galkin, Growth, optical and electrical properties of $Ca_2Si$ film grown on Si(111) and $Mg_2Si$/Si(111) substrates, Phys. Procedia 11 (2011) 95–98, https://doi.org/10.1016/j.phpro.2011.01.015.
[18] N.G. Galkin, K.N. Galkin, S.A. Dotsenko, S.A. Pyachin, I.A. Astapov, $Ca_2Si$(100) epitaxial films on the Si(111) substrate: template growth, structural and optical properties, Mater. Sci. Semicond. Process. 113 (2020), 105036, https://doi.org/10.1016/j.mssp.2020.105036.
[19] J.-I. Tani, H. Kido, Investigation of structural, elastic, and lattice-dynamical properties of $Ca_2Si$, $Ca_2Ge$, and $Ca_2Sn$ based on first-principles density functional theory, Comput. Mater. Sci. 97 (2015) 36–41, https://doi.org/10.1016/j.commatsci.2014.10.002.
[20] K.P. O'Donnel, X. Chen, Temperature dependence of semiconductor band gaps, Appl. Phys. Lett. 58 (1991) 2924–2927, https://doi.org/10.1063/1.10472310.1063/1.104723.
[21] Z. Yang, K.P. Homewood, M.S. Finney, M.A. Harry, J. Reeson, Optical absorption study of ion beam synthesized polycrystalline semiconducting $FeSi_2$, J. Appl. Phys. 78 (1995) 1958–1963, https://doi.org/10.1063/1.360167.
[22] R. Passler, Basic model relations for temperature dependencies of fundamental energy gaps in semiconductors, Phys. Status Solidi B 2001 (1997) 155–172, https://doi.org/10.1002/1521-3951(199703)200, 1<155::AID-PSSB155>3.0.CO;2-3.
[23] J.I. Pankov, Optical Processes in Semiconductors, 2nd Revised ed. edition, Dover Books on Physics, New York, 2010, pp. 22–448.
[24] M.C. Bost, J.E. Mahan, Optical properties of semiconducting iron disilicide thin films, J. Appl. Phys. 58 (1985) 2696–2703, https://doi.org/10.1063/1.335906.

[25] A. Meeder, D. Fuertes Marron, V. Tezlevan, E. Arushanov, M. Kunst, A. Rumberg, T. Schedel-Niedrig, M. Ch Lux-Steiner, Radiative recombination in CVT-grown $CuGaSe_2$ single crystals and thin films, Thin Solid Films 431–432 (2003) 214–218, https://doi.org/10.1016/s0040-6090(03)00224-4.

[26] E.K. Arushanov, E. Bucher, Ch Kloc, O. Kulikova, L. Kulyuk, A. Siminel, Photoconductivity in n-type β-$FeSi_2$ single crystals, Phys. Rev. B 52 (1995) 20–23, https://doi.org/10.1103/PhysRevB.52.20.

[27] P.W. Sparks, C.A. Swenson, Thermal expansions from 2 to 40°K of Ge, Si, and four III-V compounds, Phys. Rev. E 163 (1967) 779–788, https://doi.org/10.1103/PhysRev.163.779.

[28] J.-I. Tani, H. Kido, Lattice dynamics of $Mg_2Si$ and $Mg_2Ge$ compounds from first-principles calculations, Comput. Mater. Sci. 42 (2008) 531–536, https://doi.org/10.1016/j.commatsci.2007.08.018.

[29] M. Khalil, A. Moll, M. Godfroy, A. Letrouit-Lebranchu, B. Villeroy, E. Alleno, R. Viennois, M. Beaudhuin, Thermoelectric properties and stability of nanostructured chromium disilicide $CrSi_2$, J. Appl. Phys. 126 (2019), 135103, https://doi.org/10.1063/1.5117152.

[30] E. Arushanov, H. Lange, J. Werner, Hole mobility in p-type β-$FeSi_2$ single crystals, Phys. Status Solidi 166 (1998) 853–858, https://doi.org/10.1002/(SICI)1521-396X (199804)166:2<853::AID-PSSA853>3.0.CO;2-9.

[31] M. Wada, S. Araki, T. Kudou, T. Umezawa, S. Nakajima, Temperature dependence of the band gap in $InAs_yP_{1-y}$, Appl. Phys. Lett. 76 (2000) 2722–2725, https://doi.org/10.1063/1.126455.

[32] C. Giannini, L. Lagomarsino, F. Scarinci, P. Castrucci, Nature of the band gap of polycrystalline β-$FeSi_2$ films, Phys. Rev. B 45 (1992) 8822(R), https://doi.org/10.1103/PhysRevB.45.8822.